scientific reports

Check for updates

OPEN

Development and validation of an experimental life support system to study coral reef microbial communities

T. M. Stuij[1]✉, D. F. R. Cleary[1], R. J. M. Rocha[1], A. R. M. Polonia[1], D. A. Machado e Silva[1], J. C. Frommlet[1], A. Louvado[1], Y. M. Huang[2], N. J. De Voogd[3,4] & N. C. M. Gomes[1]✉

In the present study, we developed and validated an experimental life support system (ELSS) designed to investigate coral reef associated bacterial communities. The microcosms in the ELSS consisted of coral reef sediment, synthetic seawater, and specimens of five benthic reef species. These included two hard corals *Montipora digitata* and *Montipora capricornis*, a soft coral *Sarcophyton glaucum*, a zoanthid *Zoanthus* sp., and a sponge *Chondrilla* sp.. Physicochemical parameters and bacterial communities in the ELSS were similar to those observed at shallow coral reef sites. Sediment bacterial evenness and higher taxonomic composition were more similar to natural-type communities at days 29 and 34 than at day 8 after transfer to the microcosms, suggesting microbial stabilization after an initial recovery period. Biotopes were compositionally distinct but shared a number of ASVs. At day 34, sediment specific ASVs were found in hosts and visa versa. Transplantation significantly altered the bacterial community composition of *M. digitata* and *Chondrilla* sp., suggesting microbial adaptation to altered environmental conditions. Altogether, our results support the suitability of the ELSS developed in this study as a model system to investigate coral reef associated bacterial communities using multi-factorial experiments.

Coral reefs are among the most diverse and productive of marine ecosystems and are home to an estimated 25% of known marine species[1]. They also provide important economic services including coastal protection, tourism and fisheries[1–3]. However, anthropogenic perturbations are increasingly affecting the health and resilience of coral reefs[4–6]. For example, the frequency of extreme El Niño southern oscillation (ENSO) events has increased over the past decades[7–9]; this has been linked to larger-scale and more severe coral bleaching events[4,10,11]. Given the above, it is important to understand how coral reef organisms respond to environmental perturbations, particularly those related to predicted increases in temperature and UVB intensity and their relationship with large-scale processes[12].

In coral reef ecosystems, understanding the impact of multiple environmental factors on community dynamics is challenging due to the complex interplay between these factors[13]. Randomised controlled microcosm experiments offer a valuable approach to distinguish correlation from causation by reducing environmental complexity. Such experiments allow for hypothesis testing and the examination of independent and interactive effects of different environmental factors[14–17]. This facilitates a more mechanistic understanding of the relationship between specific environmental factors and the response variable or variables of interest[14,15,18]. Moreover, microcosm-based studies offer a way to study organismal responses to specific and controllable treatments[19,20], which may not be possible in a natural setting.

In recent years, a growing body of studies have highlighted the importance of reef microbial communities for coral reef resistance and resilience to environmental perturbations[21–24]. These communities play important roles in biogeochemical cycling, pollutant degradation, coral nutrition and defense against pathogens and predators[25–30]. Both non-host (e.g., in sediment and seawater) and host-associated communities, have been shown to respond to spatial and environmental processes including large and local-scale perturbations[15,31–33]. However, controlled experiments, which include microbial communities from various reef biotopes are scarce.

[1]Centre for Environmental and Marine Studies (CESAM) and Department of Biology, University of Aveiro, Campus Universitário Santiago, 3810-193 Aveiro, Portugal. [2]National Penghu University of Science and Technology, Magong, Taiwan. [3]Naturalis Biodiversity Center, Leiden, the Netherlands. [4]Institute of Biology (IBL), Leiden University, Leiden, the Netherlands. ✉email: tamarastuij@ua.pt; gomesncm@ua.pt

In the current study, we developed and validated an experimental life support system (ELSS), designed to perform multi-factorial experiments to investigate coral reef associated bacterial communities of non-host and host associated biotopes. We monitored physical and chemical parameters, assessed coral photosynthetic efficiency and investigated sediment, water, and host-associated bacterial communities. Subsequently, we validated the system by comparing the conditions and bacterial communities in the ELSS with those occurring in natural coral reef environments.

Methods

ELSS design

The design of the ELSS developed in this study was based on a microcosm system previously developed to assess the effects of global climate change and environmental contamination on sediment communities[14]. In the current study, the ELSS included two frames of 16 microcosms (glass aquaria, 23 cm in height, 16 cm length and 12 cm width). Each individual microcosm was connected to another aquarium (referred to as reservoir, 30 cm in height, 12 cm length and 12 cm width); see Fig. 1. The microcosms and reservoirs contained outflow-holes (two centimetres in diameter) positioned 3 and 5 cm below the top of the glass, respectively. Each reservoir was equipped with a small hydraulic pump (compactON 300, EHEIM) to pump water out of the microcosm into the reservoir, where subsequently the water level would rise and flow out into the accompanied microcosm with a constant flow rate of approximately 8.64 ml/s (s = 0.66 ml/s). Each reservoir-microcosm unit contained a functional water volume of approximately 5 L.

Water changes, temperature, light and aeration control system

Water was renewed daily by replacing 1 L of water with newly prepared synthetic seawater. Synthetic seawater was prepared by mixing coral reef salt (including associated oligo-nutrients) (CORAL PRO SALT, Red Sea) with deionized water (produced in a four-stage reverse osmosis unit—V2Pure 360) to a concentration of 35 ppt. To obtain sufficient mixing, the synthetic seawater was prepared in a large container supplied with a recirculating pump at least 12 h prior to addition to the reservoirs.

Temperature was regulated using water bath tanks, each of which surrounded four microcosms[14] (Fig. 1). For 34 days, water temperature was kept at 28 °C using heaters equipped with an internal thermostat (V2Therm 100 Digital heater). This temperature was chosen to resemble water temperatures previously measured at Pacific reefs[34,35]. The modular design of the ELSS set up enables randomized split-plot design experiments, whereby each plot consists of four microcosms of equal temperature.

Lighting was controlled by four fully programmable luminaire systems (Reef—SET, Rees, Germany), each holding eight fluorescent lamps[14]. During the current experiment, four UV fluorescent tubes (SolarRaptor, T5/54W) and four full spectra fluorescent tubes (ATI AquaBlue Special, T5/54W) were connected alternately. To simulate photoperiod conditions of tropical latitudes, the lamps were programmed to a 12 h diurnal light cycle with light intensity varying from $2.61*10^{-3}$ J cm^{-2} s^{-1} in the morning to $8.82*10^{-3}$ J cm^{-2} s^{-1} at mid-day (measured using a Fibre optic probe positioned at the water surface, Flame spectrometer, Ocean Optics). The total light energy transmitted during the day equalled 256 J cm^{-2} day^{-1}, of which 97.7% came from the photoactive radiation (PAR) wavelengths (300–700), 1.85% from the UVA wavelengths (315–400) and 0.43% from the UVB wavelengths (280–315). Photosynthetic photon flux density (PPFD, mol photons m^{-2} s^{-1}) at the sediment–water interface was measured using an underwater PAR meter (MQ-510 PAR/Quantum-Meter Underwater, Apogee, USA). A total of 3.47 ± 0.68 mol photons m^{-2} d^{-1} reached the sediment surface. A transparent polyester film (Folanorm SF-AS, Folex coating, Köln, Germany) was used to block UVB light (290–320 nm)[36,37]. This film absorbed 90% of the UVB irradiance, 31% of UVA and 9% of PAR irradiance. A detailed figure of the light spectrum can be found in Supplementary Fig. 1. When the ELSS is used to investigate the effects of UVB on coral reef organisms, this film can be removed from the microcosms. All microcosms were connected to an air pump

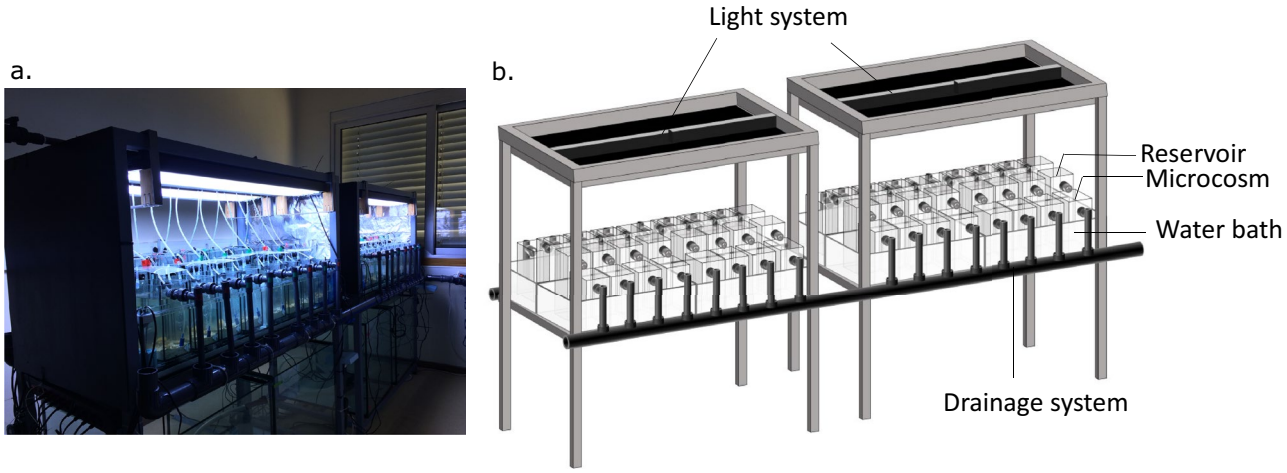

Figure 1. Picture (**a**) and graphical representation (**b**) of the experimental life support system.

(530L/h, Resun) providing equal and constant aeration in each microcosm via a small hose and a diffuser stone (1.5 cm in diameter, 3 cm in length).

Coral reef sediment and organisms

Approximately 3 cm of sediment, equivalent to 700 g wet weight per microcosm, was added to the bottom of each microcosm. This sediment consisted of a mixture of commercially available (Reef Pink dry aragonite sand, Red Sea) and natural coral reef sediment. Natural sediment was collected from a coral reef south of Fongguei, Penghu Islands, Taiwan (22° 19′ 50.5″ N 120° 22′ 19.8″ E). Within 5 days, the sediment was transported to our laboratory in Portugal in a coolbox and stored at 4 °C until use. The commercial sediment was washed and sterilized. Sterilization was performed by 3 times autoclavation at 121 °C for 20 min[38]. 20 kg of sterilized commercial sediment was spiked with 4 kgs of natural coral reef sediment, which equates to a 1 to 6 ratio of live to sterilized sediment. The sediments were thoroughly mixed and added to the microcosms.

The ELSS was left to stabilize with spiked reef sediment and synthetic seawater for the first eight days of the experiment. Subsequently, five reef animal species were added, after which the system ran for an additional 26 days. Overall, the system ran continuously for 34 days. The species used in the ELSS included two hard corals, *Montipora digitata* (Dana, 1846) and *Montipora capricornis* (Veron 1985), one soft coral, *Sarcophyton glaucum* (Quoy & Gaimard, 1833), one zoanthid, *Zoanthus* sp., and one sponge, *Chondrilla* sp.. All animals used in this study were previously grown in aquaria at ECOMARE (CESAM, University of Aveiro, Portugal)[39]. A detailed explanation of the fragmentation process of the organisms can be found in the Supplementary material.

Physical and chemical analysis

Water quality was monitored daily by measuring temperature, pH, dissolved oxygen and salinity (Multi 3420 multimeter, WTW GmbH, Weilheim, Germany). Samples to determine dissolved inorganic nutrient concentrations (nitrate NO^{3-}; nitrite NO^{2-} ammonium NH^{4+}, and phosphate PO_4^{3-}) in the water column were taken every 7 days, using disposable syringes (50 ml), and were measured immediately, according to the Sali test kit protocol (colorimetric method test kit, salifert, Aquarium Masters). Additionally, we analysed dissolved inorganic nutrients (nitrate NO^{3-}; nitrite NO^{2-}; ammonium NH^{4+}; phosphate PO_4^{3-}; and sulphate SO_4^{2-}) and total organic carbon (TOC) concentrations from samples of ELSS sediment porewater after eight, 28 and 34 days. A detailed description on the methodology of these measurements can be found in the Supplementary material.

In vivo chlorophyll fluorescence analysis

Chlorophyll fluorescence of the corals and zoanthid was measured at days 0 and 34 in vivo using a pulse amplitude modulation (PAM) fluorometer (Walz™). Fluorescence was measured in dark-adapted samples (for 20 min), with Junior PAM and WinControl3 software (Walz™). Saturating light pulses (450 nm) were performed perpendicularly to the sample surface, with a 1.5 mm fibre optic. The maximum quantum yield (Fv/Fm) of photosystem II was calculated as $\mathrm{Fv/Fm} = \frac{Fm-F0}{Fm}$. Fv/Fm ratios reflect the efficiency of PSII (photosynthetic efficiency) of coral-algal symbionts. Reductions in Fv/Fm ratios are an indicator of increased stress experienced by algae and their coral hosts[40,41].

Bacterial community analysis

Sampling and DNA extraction

Sediment, water and porewater samples were collected after 8, 29 and 34 days of four independent microcosms. Reef animals were sampled at the end of the experiment (after 34 days) and rinsed with filtered (0.22-µm pore size) synthetic seawater to remove loosely attached organisms. Additionally, samples from the natural sediment collected in Taiwan and from benthic reef animals prior to addition to the microcosms (hereafter referred to as "Pre") were preserved for further analysis (see Fig. 2). During sediment collection in Taiwan, three sediment samples of approximately 20 g were collected in situ and immediately preserved in 96% alcohol. From the microcosms, a composite sediment sample consisting of four smaller subsamples (~ 3 g each) was obtained using a sterilized scoop. The subsamples were taken haphazardly from each microcosm (1 cm of surface sediment with a ~ 2 cm diameter). One sample from the sterilized commercial sediment was obtained as control for ELSS contamination with environmental DNA[42] and sample collection[43].

Water was sampled by filtering 250 ml of water through a Millipore® Isopore polycarbonate membrane filter (0.22-µm pore size; Millipore®) using a vacuum filtration system. All sediment samples, whole membrane filters and reef organisms were frozen at − 80 °C until DNA extraction.

DNA extraction and sequence analysis

Details on DNA extraction, library preparation and sequencing can be found in the Supplementary material. Briefly, PCR-ready genomic DNA was isolated from all samples using the FastDNA® SPIN soil Kit (MPbiomedicals) following the manufacturer's instructions. From the extracted DNA, the V3/V4 variable region of the 16S rRNA gene was amplified with Illumina Nextera XT overhang adapters in a dual-barcoding PCR library preparation approach. The prepared DNA was subsequently sequenced at a commercial company (Baseclear, Leiden, The Netherlands) on the Illumina MiSeq platform using 2 × 300 bp paired-end sequencing (Illumina MiSeq PE300). Three negative control samples were included to detect possible contamination during library preparation and sequencing. Sequences from each end were paired following Q25 quality trimming and removal of short reads (< 150 bp). The DNA sequences generated in this study can be downloaded from NCBI BioProject Id PRJNA904682.

The generated 16S rRNA gene amplicon libraries were imported into QIIME2[44]. Within the QIIME2 environment, forward and reverse sequences were trimmed to a length of 245 and 200 nt, respectively, using the DADA2

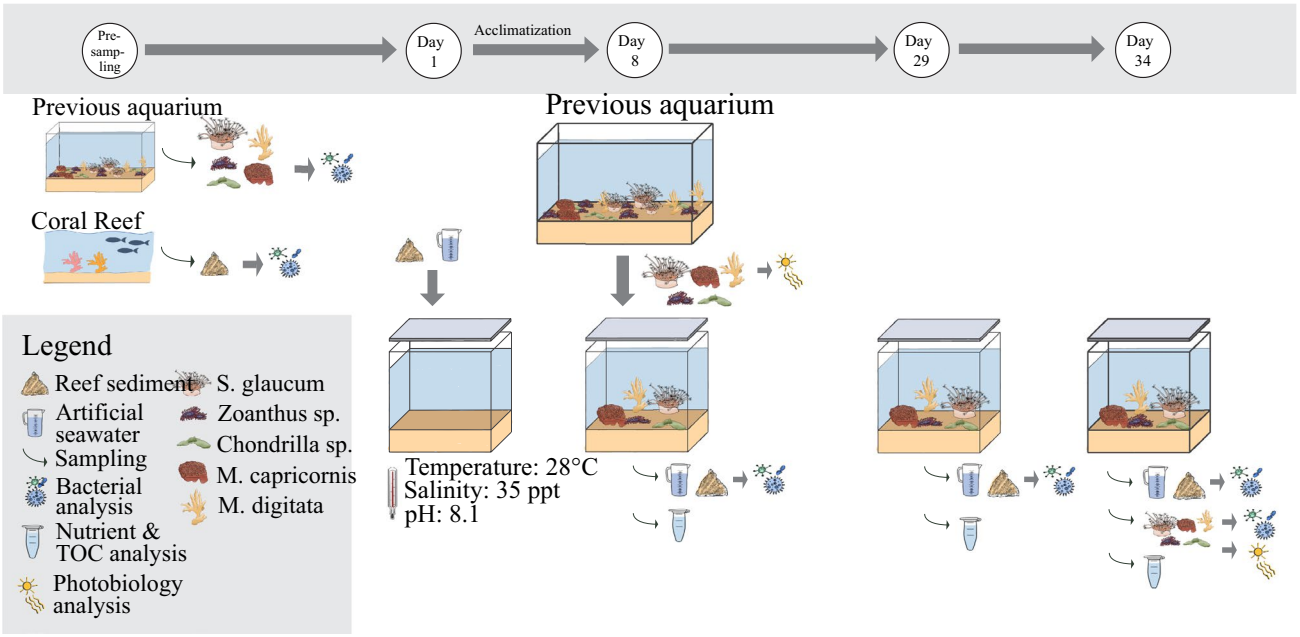

Figure 2. Graphical summary of the experimental set-up.

plugin[45]. The DADA2 analysis produced a quality filtered table of all amplicon sequence variants (ASVs), a fasta file of representative sequences, and a table summarising the denoising statistics. Following this, the QIIME2 feature-classifier plugin with the extract-reads option was used to extract reads from the Silva database with the silva-138-99-seqs.qza file as input and the forward and reverse PCR primers as parameters. This produced a file of reference sequence reads, which was used as input for the feature-classifier plugin with the fit-classifier-naive-bayes option. The plugin trained a Naive Bayes classifier and produced a classifier file (classifier.qza) as output. The feature-classifier plugin was then used with the classify-sklearn alogrithm using the representative sequences file generated by the DADA2 analysis as input, which produced a table with taxonomic assignments for all ASVs. Mitochondria, chloroplasts, and ASVs classified as Eukaryota were filtered out using the QIIME2 taxa plugin with the filter-table method. The ASV and taxonomy tables were later merged in R. After quality control and removal of singletons, chloroplasts and mitochondria, the total dataset of sediment, water and host bacterial samples consisted of 1,549,657 sequences and 13,711 ASVs. The ASV count table and a fasta file containing all sequences are presented in Supplementary Tables 1 and 2, respectively.

Subsequently, we removed all ASVs classified as Archaea and ASVs that were unassigned at the phylum level. We also removed ASVs, which occurred in the triple-autoclaved commercial sediment (control for sampling and eDNA contamination) and negative controls used for sequencing (removed ASVs are listed in Supplementary Table 3). Overall, the removed ASVs were assigned to known contaminants, for example, the genera *Ralstonia, Burkholderia-Caballeronia-Paraburkholderia, Reyranella, Bacillus* and *Bradyrhizobium*[46–48]. After these filtering steps, we removed two samples with low read counts before subsequent analysis; E2G4 (339 sequences) and E2Z1 (1004 sequences). The resulting dataset consisted of 62 samples, 1,414,326 sequence reads and 13,225 ASVs.

The 50 most abundant ASVs were referenced against the NCBI nucleotide database using NCBI Basic Local Alignment Search Tool (BLAST)[50]. BLAST identifies locally similar regions between sequences, compares sequences to extant databases and assesses the significance of matches. Each BLAST run produces a list of results between the sequence in question (the query sequence), obtained from selected ASVs in the present study, and target sequences in the NCBI nucleotide database.

Predicted metagenomic analysis

To analyse the putative functional profile of the bacterial communities, we used the Tax4Fun2 library[49] in R. Tax4Fun2 predicts the metagenomic content of the samples using the KEGG (Kyoto Encyclopedia of Genes and Genomes) database. Output of Tax4Fun2 consists of a table of functional counts for individual pathways and KEGG orthologs (KOs). Note that because of functional overlap, some KEGG orthologs (KOs) can be represented in multiple pathways. Tax4Fun2 also produces output on the amount of ASVs and sequences used in the prediction for each sample. This can vary among samples depending on the availability of closely-related, sequenced genomes available in the Tax4Fun2-supplied (Ref100NR) database. Note that the Tax4Fun2 results as presented are predictive and thus provide information on potential enrichment and putative function as opposed to measuring actual gene presence/expression and function.

Statistical analysis

We tested for significant differences among sampling events in SO_4^{2-} and TOC concentrations, and Fv/Fm ratios. Histograms revealed significant deviations from normality. The distributions continued to deviate significantly following logarithmic and square root transformations. We, therefore, tested for significant differences

in SO_4^{2-} and TOC concentrations, and Fv/Fm ratios among sampling events using a repeated measures permutational analysis of variance with the adonis2() function (Vegan package) in R. In the function, the method was set to "euclidean" and permutations to "999".

To analyse the bacterial community data, a table containing the ASV counts was imported into R. The ASV table was used to analyse the impact of the microcosm system on bacterial diversity, composition and higher taxon abundance. Diversity indices were obtained using the rarefy() and diversity() functions from the vegan package[51] package in R. Evenness was calculated by dividing Shannon's H' by the log of the number of ASVs in each sample. Differences in diversity indices, higher taxon abundances and selected KEGG pathways were investigated using an analysis of deviance (glm() function of the R package stats). In the function, we set the family argument to "quasipoisson" (richness) or "quasibinomial" (evenness, higher taxa and KEGG pathways), which is appropriate when analysing proportional data and allowed us to model overdispersion. Using the glm model, we tested for significant variation using the anova() function in R with the F test, which is most appropriate when dispersion is estimated by moments as is the case with quasibinomial fits. We subsequently used the emmeans() function in the emmeans library[52] to perform multiple comparisons of mean abundance among sample events using the false discovery rate (fdr) method in the adjust argument.

Variation in bacterial composition among groups (time points and biotopes) was visualized with Principal Coordinates Analysis (PCO). For the PCO, the ASV table was rarefied to the minimum sample size using the rrarefy() function of the R package vegan (4818 sequences in the present study). For compositional analyses, the ASV table was transformed using the decostand() function in vegan with the method argument set to 'Hellinger'. With this transformation, the ASV table is adjusted such that subsequent analyses preserve the chosen distance among objects (samples in this case). The ASV table was transformed because of the inherent problems with the Euclidean-based distance metric, which is frequently used in cluster analyses[53]. A distance matrix was subsequently created with the vegdist() function in vegan using the Hellinger-transformed ASV table as input and the method argument set to "euclidean". Subsequently, we used the cmdscale() function of the R package stats with the Hellinger transformed distance matrix as input. We quantified the degree of similarity in bacterial communities between Pre (environmental) sediments and sediments sampled at days 8, 29 and 34 by calculating their mean dissimilarity using the meandist() function in the R package vegan with the dist argument set to the Hellinger transformed distance matrix. A permutational anova was performed using the adonis2() function of the R package vegan to test for significant differences in composition among sampling events per biotope (999 permutations). Additionally, we analysed the variance of host-associated bacterial communities within Pre and day 34 samples by first computing a Bray–Curtis transformed dissimilarity matrix using the decostand() and vegdist() functions (method set to "Bray"), which was subsequently used to compute distances to centroids using the betadisper() function in the R package vegan. Detailed descriptions of the functions used here can be found in R (e.g., ?cmdscale) and online in reference manuals (http://cran.rproject.org/web/packages/vegan/index.html). To acquire information on the connectivity between sediment and host-associated bacterial communities, we analysed the number of ASVs shared among host and sediment biotopes at Pre versus day 34 conditions using the function upset() in the R package UpSetR. Lists of ASVs detected in each sample group were used as input. Lists were computed after rarefaction of the ASV table and only ASVs with ≥ 0.1% were included.

Results

Physical and (bio)chemical analysis

Water temperature varied from a minimum of 26.4 ± 0.65 °C in the morning to a maximum of 28.3 ± 0.83 °C in the afternoon. Dissolved oxygen levels varied over the day from a minimum of 7.83 ± 0.50 mg L^{-1} in the morning to a maximum of 8.60 ± 0.45 mg L^{-1} in the afternoon. In line with variation in oxygen concentrations, pH varied over the day from 8.06 ± 0.04 to 8.17 ± 0.08 (Supplementary Fig. 2). During the course of the experiment, NO_3^-, NO_2^-, NH_4^+ and PO_4^{3-} concentrations in the water column and pore water remained below detection limits (< 0.2, < 0.01, < 0.15 and < 0.05 mg L^{-1}, respectively). There was a significant reduction in the concentration of pore water SO_4^{2-} from 2940.0 ± 16.33 mg L^{-1} at the first measurement to 2520.0 ± 40.82 mg L^{-1} at the end of the experiment (repeated measures PERMANOVA, $F_{2,9} = 18.89$, $R^2 = 0.81$, $P = 0.035$, Supplementary Fig. 2). Although not significant, TOC increased from 1.77 ± 0.18 to 4.97 ± 2.59 mg C L^{-1} at the end of the experiment (repeated measures PERMANOVA, $F_{2,9} = 3.28$, $R^2 = 0.42$, $P = 0.15$, Supplementary Fig. 2).

Coral photosynthetic efficiency

Fv/Fm ratios significantly increased from 0.46 ± 0.01 at day 0 to 0.53 ± 0.01 at day 34 in *M. digitata* (PERMANOVA: $F_{1,6} = 148.56$; $R^2 = 0.96$; $P = 0.031$). Fv/Fm ratios increased non-significantly from 0.52 ± 0.01 to 0.54 ± 0.02 in *M. capricornis* (PERMANOVA: $F_{1,6} = 3.50$; $R^2 = 0.37$; $P = 0.157$) and non-significantly from 0.52 ± 0.04 to 0.59 ± 0.03 in *S. glaucum* (PERMANOVA: $F_{1,6} = 10.41$; $R^2 = 0.63$; $P = 0.062$); in *Zoanthus* sp. Fv/Fm ratios decreased non-significantly from 0.51 ± 0.02 to 0.44 ± 0.07 (PERMANOVA: $F_{1,6} = 3.46$; $R^2 = 0.37$; $P = 0.174$).

Bacterial community analysis

Diversity

Richness and evenness were highest within sediment bacterial communities, but varied among sampling events (Table 1 and Supplementary Table 4). In sediment, richness first increased non-significantly from day 8 to day 29 and subsequently declined significantly from day 29 to day 34. Evenness was significantly lower at day 8 than Pre, day 29 and day 34 samples. In water, richness and evenness both significantly increased from day 8 to day 29 and remained stable from day 29 to 34. Richness and evenness did not vary significantly among sampling events in host biotopes, with the exception of *M. digitata*, in which we observed a significantly lower evenness in Pre compared to day 34 samples.

Richness	Pre	D8	D29	D34
Sediment	1065 ± 87	1023 ± 120	**1469 ± 126**	**621 ± 447**
Water	–	126 ± 16	**321 ± 44**	298 ± 69
M. digitata	259 ± 144	–	–	296 ± 147
M. capricornis	470 ± 48	–	–	377 ± 82
S. glaucum	289 ± 204	–	–	340 ± 118
Zoanthus sp.	120 ± 16	–	–	191 ± 152
Chondrilla sp.	58 ± 13	–	–	56 ± 5
Evenness				
Sediment	0.95 ± 0.00	**0.85 ± 0.04**	**0.94 ± 0.01**	0.91 ± 0.01
Water	–	0.50 ± 0.04	**0.71 ± 0.02**	0.66 ± 0.06
M. digitata	0.67 ± 0.11	–	–	**0.85 ± 0.05**
M. capricornis	0.83 ± 0.05	–	–	0.77 ± 0.03
S. glaucum	0.66 ± 0.05	–	–	0.64 ± 0.09
Zoanthus sp.	0.88 ± 0.01	–	–	0.79 ± 0.13
Chondrilla sp.	0.65 ± 0.02	–	–	0.67 ± 0.04

Table 1. Mean and standard deviations of rarefied richness & evenness. Values which significantly varied from the previous sampling event are indicated in bold ($P < 0.004$, GLM with emmeans, see supplementary Table 4).

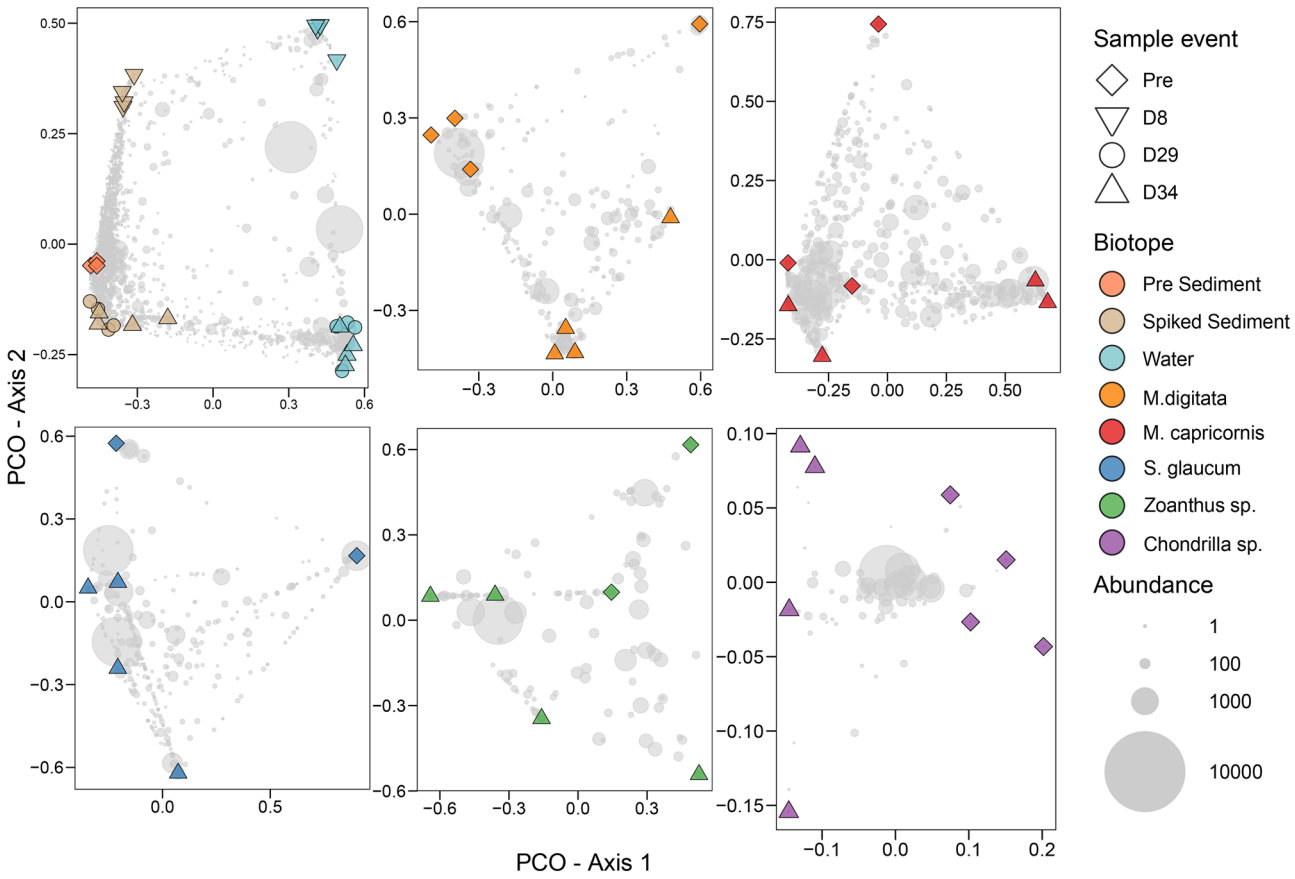

Figure 3. Ordinations showing the first two axes of the principal coordinates analysis (PCO) of prokaryote ASV composition for sediment and water, and each host species separate. Light grey symbols represent operational taxonomic unit (ASV) scores with the symbol size representing their abundance (number of sequence reads). Supplementary Table 5 lists eigenvalues, the total variation explained and results of the PERMANOVA for each ordination.

Ordination analysis (Fig. 3) showed that sampling event was a significant predictor of variation in the bacterial community composition of the sediment, water, and the host organisms *M. digitata* and *Chondrilla* sp. (PERMANOVA: $P < 0.05$, Supplementary Table 5). When grouped together, variance among samples of host-organisms was similar in Pre compared to day 34 conditions, as evidenced by similar distances to centroids (Pre: 0.625 ± 0.035; day 34: 0.632 ± 0.045, Supplementary Fig. 3). Samples clustered according to their host-species (PERMANOVA, $F_{4,30} = 6.93$; $R^2 = 0.48$; $P = 0.001$). In water and sediment, the main axis of variation separated samples according to biotope whereas the second axis separated water and sediment samples collected at day 8 from Pre, day 29 and day 34 samples. However, the mean bacterial community dissimilarity was marginally higher between Pre and day 34 (89%) compared to Pre and day 8 and 29 samples (85 and 86%, respectively).

Higher taxonomic composition

The most abundant phyla across the complete dataset were Proteobacteria (4156 ASVs, 751,894 sequences), Planctomycetota (2214 ASVs, 138,421 sequences), Bacteriodota (1634 ASVs, 84,631 sequences), Cyanobacteria (221 ASVs, 78,311 sequences), Actinobacteriota (485 ASVs, 59,621 sequences), Firmicutes (215 ASVs, 54,368 sequences), Verrumicrobiota (1112 ASVs, 52,766 sequences) and Patescibacteria (490 ASVs, 45,003 sequences) (Supplementary Table 6). Of these, Cyanobacteria were particularly abundant in *Chondrilla* sp., whereas Patescibacteria were most prevalent in water communities (Fig. 4).

The relative abundances of the most abundant phyla and proteobacterial classes varied significantly among sampling events in water and sediment communities (Fig. 4), whereas no significant differences were observed between sampling events in host organisms (Pre and day 34) (emmeans, Supplementary Table 7). In sediment, Desulfobactereota, Firmicutes and Spirochaetota abundances were significantly ($P < 0.0004$) lower at days 8, 29 and 34 compared to Pre samples, whereas the abundance of Dadabacteria was significantly higher at days 29 and 34 compared to Pre and day 8 (emmeans, Supplementary Table 7). Chloroflexi abundance first declined significantly from Pre to day 8, increased significantly from day 8 to 29, and did not vary significantly from day 29 to 34, whereas the inverse held for Gammaproteobacteria (emmeans, Supplementary Table 7). In water, the abundance of Verrucomicrobiota and Planctomycetota significantly increased from day 8 to 34 (emmeans, Supplementary Table 7).

Shared ASVs among sediment and host-organisms in Pre and ELSS conditions

All biotopes consisted of both biotope-specific ASVs alongside ASVs which were shared among two or more biotopes (Supplementary Fig. 4–6). Among host organisms, there were a total of 183 shared ASVs in Pre and 277 shared ASVs in day 34 samples. A total of 168, 137 and 157 ASVs were detected in both Pre sediments and sediments at days 8, 29 and 34, respectively. At day 34, 169 ASVs were shared between sediment and host-biotopes. Of these, 18 were also detected in both Pre sediments and hosts, whereas 37 ASVs were only detected in Pre host samples and 36 ASVs in Pre sediments.

Most abundant ASVs and their closest relatives

Of the 50 most abundant ASVs, five were recorded in sediment across all sample events (Fig. 5). These ASVs were assigned to the genera *Ruegeria* (ASVs 5, 25), *Methyloceanibacter* (ASV-36), *Filomicrobium* (ASV-37) and the family Geminicoccaceae (ASV-67). A more in-depth analysis showed that ASVs 5 and 25 were related to *R. lacuscaerulensis* isolates (100% sequence similarity), whereas the other three ASVs were related to uncultured organisms, previously detected in marine sediment (ASV-67), intertidal outcrops (ASV-37), and the coral *Galaxea fascicularis* (ASV-36, > 99% sequence similarity, Supplementary Table 8). With the exception of ASV-67, all of these ASVs were also found in water (ASVs 5 and 36) and/or host organisms (ASVs 5, 25, 36, 37) across sampling events.

Ten ASVs, assigned to the Alpha- and Gammaproteobacteria (ASVs 2, 11, 19, 23, 39, 41, 52, 55, 3 and 142) were consistently abundant in sediment at days 8, 29 and 34 but were not detected in Pre sediment. They also occurred in water and invertebrate hosts at various sampling events. ASVs 2, 11, 52 and 142 were related (100% sequence similarity) to isolates classified as *Tritonibacter litoralis*, *Leisingera* sp., *Ruegeria* sp. strain and *Alteromonas* sp. detected in seawater, a coral, marine sediments and estuarine soil, respectively. ASVs 3, 19, 23, 39, 41 and 55 were related to (> 97% sequence similarity) uncultured organisms detected in seawater, the coral *Fungia granulosa*, the coral *Alcyonium digitatum*, the sponge *Haliclona* sp., endolithic communities and marine sediment, respectively. Three ASVs (30, 43 and 186), assigned to the classes Gracilibacteria and ABY1, were not detected in sediment and host Pre samples, but were abundant across water and sediment at days 29 and 34 and associated with several invertebrate hosts at day 34. Additionally, eleven of the 50 most abundant ASVs showed a biotope specific association (only recorded in a single biotope). For example, ASV-42 (*Entoplasmatales*) was only recorded in *S. glaucum*, ASV-10 (*Endozoicomonas*) in *Zoanthus sp.*, and ASVs 26 (BD2-11 terrestrial group) and 32 (Cyanobiaceae) in *Chondrilla sp.*. These ASVs were similar to uncultured organisms previously detected in the sea anemone *Nematostella vectensis*, a deep-sea octocoral, and the sponges *Xestospongia muta* and *Haliclona* sp., respectively (Supplementary Table 8).

Predicted functional analysis

The fraction of ASVs and sequences used in the prediction of metagenomic content varied from $12.9 \pm 1.5\%$ ASVs and $22.3 \pm 1.0\%$ of sequences in day 29 sediment samples to $43.4 \pm 11.2\%$ ASVs and $57.4 \pm 2.04\%$ sequences in Pre *M. digitata* samples (Supplementary Table 9). The predicted relative abundances of 7 of the 12 tested KEGG categories remained relatively stable across all sampling events. Variation was observed in the nitrogen metabolism category, which significantly declined from Pre to day 8, but increased from day 8 to days 29 and 34 to similar values found in Pre sediments ($P < 0.0006$, Fig. 6 and Supplementary Table 10). Additionally, predicted

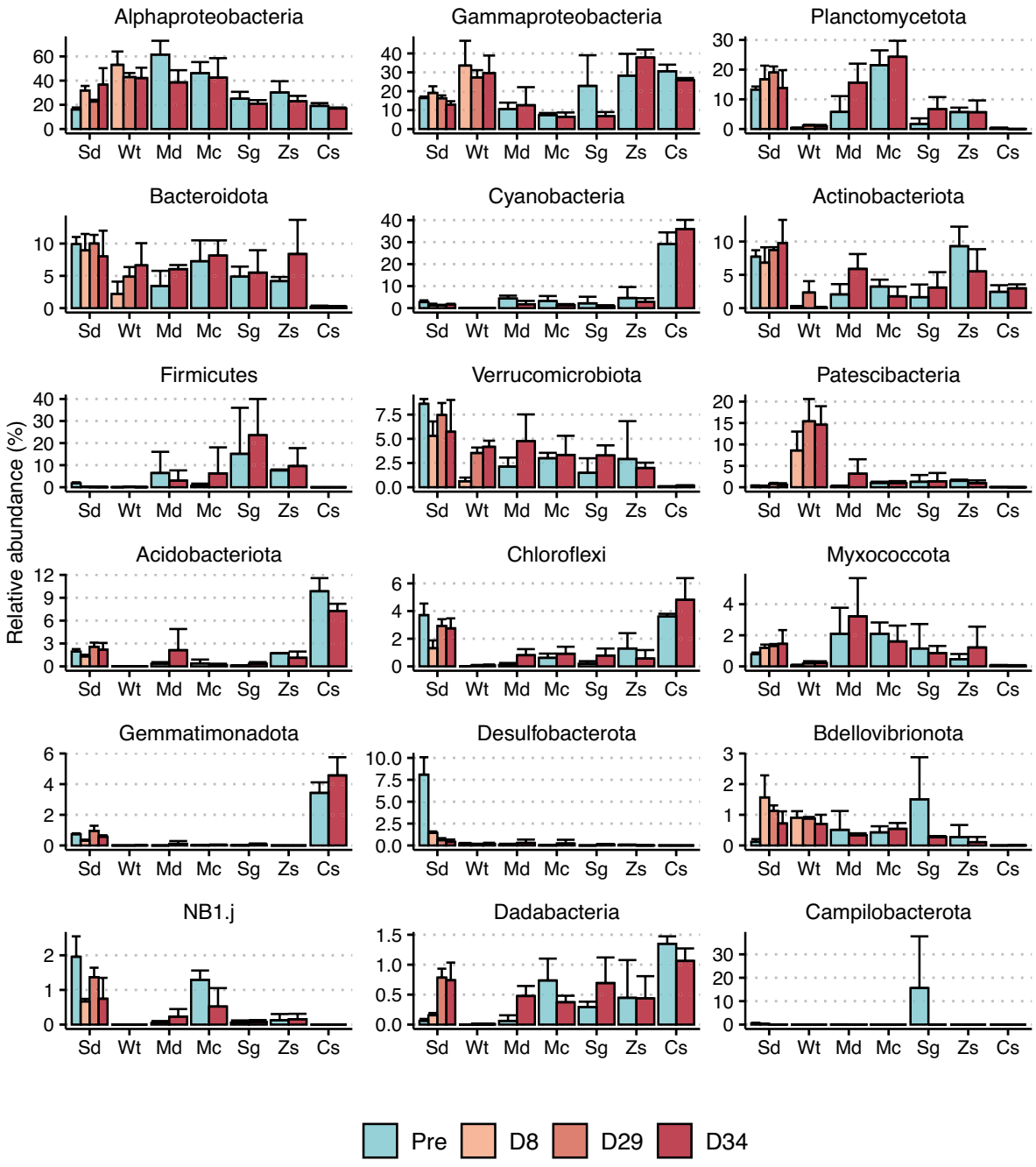

Figure 4. Mean relative abundance of the most abundant proteobacterial classes and phyla of biotopes at the different sample events. Error bars represent standard deviations of the mean. Sd: sediment, Wt: water, Md: *M. digitata*, Mc: *M. capricornis*, Sg: *S. glaucum*, Zs: *Zoanthus* sp., Cs: *Chondrilla* sp.

gene count abundances of the cAMP signalling and two-component system categories significantly ($P < 0.0006$) decreased, and the carbon metabolism and quorum sensing categories significantly increased from Pre to day 8 and thereafter remained relatively stable from days 8 to 34 (emmeans, Supplementary table 9). In water, 6 of the categories remained stable. Variation was observed among the carbon metabolism, secondary metabolites and antibiotic biosynthesis categories, which increased from day 8 to 34, whereas the quorum sensing category decreased (emmeans, Supplementary Table 10). The terpenoid backbone biosynthesis category increased from day 8 to 29, but there was no significant difference between day 8 and 34. The cAMP signalling category significantly increased from day 8 to 29 and subsequently significantly decreased from day 29 to 34 (emmeans, Supplementary Table 10). In host biotopes, none of the functional categories investigated differed significantly between sampling events.

Figure 5. Relative abundance of the 50 most abundant ASVs, which are colour-coded according to their phylum-level classification. The circle size of the ASV is proportional to the mean percentage of sequences per biotope and sampling event. The y-axis lists the ASVs with their respective id number. Sd: sediment, Wt: water, Md: M. digitata, Mc: *M. capricornis*, Sg: *S. glaucum*, Zs: *Zoanthus* sp., Cs: *Chondrilla* sp.

Discussion

The current study aimed to develop and validate an ELSS to study coral reef microbial communities under controlled conditions. To this end, we assessed bacterial community composition (sediment, water, and host-associated communities), coral photosynthetic efficiency, and physicochemical parameters (e.g., salinity, pH, temperature, PAR and UV light, inorganic nutrients and DOC) within the ELSS. Sediment bacterial communities within the microcosms were compared to those in natural environmental sediments. Additionally, we compared host-associated bacterial communities within the ELSS to those in their original culture aquarium to examine the impact of transplantation.

Physicochemical parameters, photosynthetic efficiency and their resemblance to natural conditions.

Average values of the water temperature, dissolved oxygen, pH and salinity in the microcosms fell within the range of values measured at shallow coral reef sites[34,54,55]. Daily fluctuations were observed among water

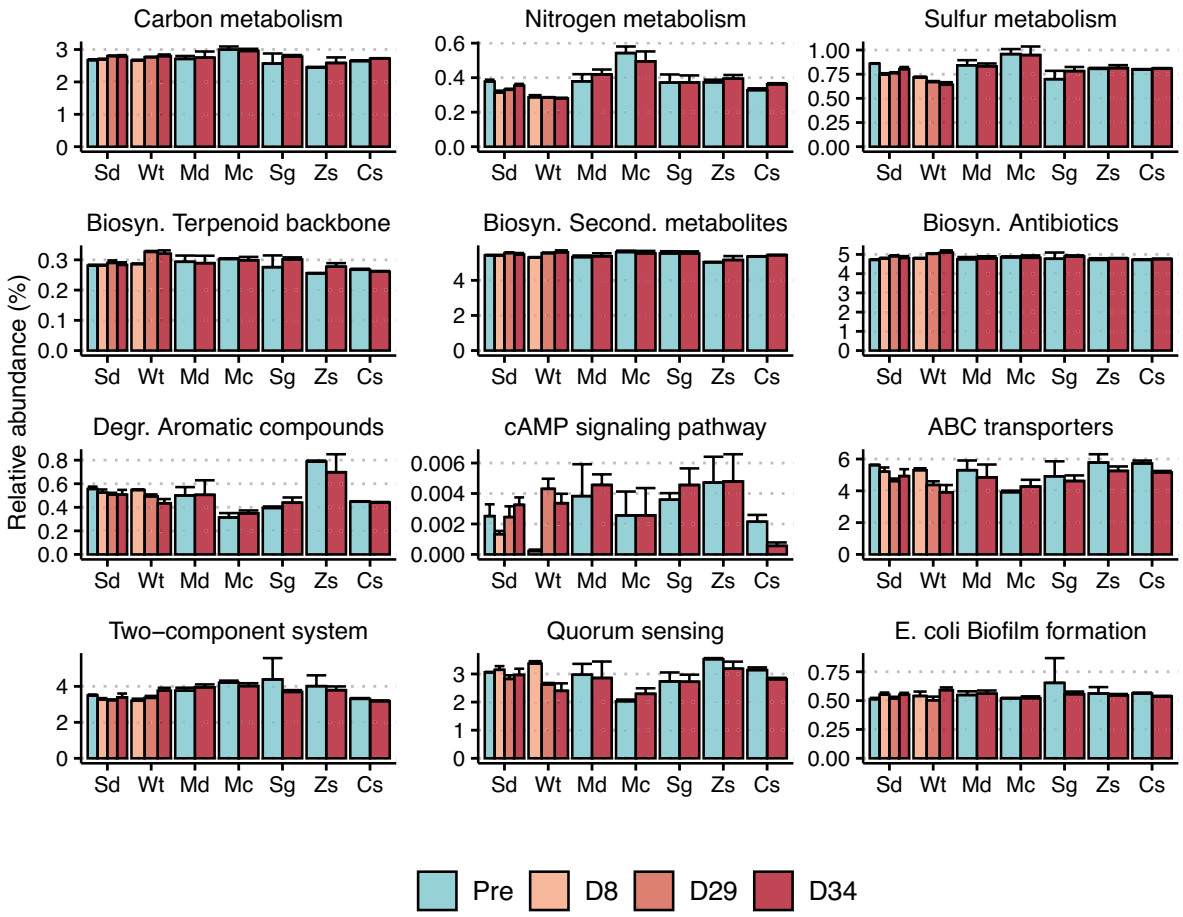

Figure 6. Predicted mean relative gene count abundance of the KEGG level 1 categories of biotopes at the different sample events. Error bars represent standard deviations of the mean. Sd: sediment, Wt: water, Md: *M. digitata*, Mc: *M. capricornis*, Sg: *S. glaucum*, Zs: *Zoanthus* sp., Cs: *Chondrilla* sp.

temperatures (increased by 2 degrees during the course of the day), oxygen and pH (higher in the morning and lower in the afternoon). At reefs, similar temperature fluctuations have been observed due to sun exposure[34,54], whereas oxygen and pH can fluctuate as a result of net-photosynthesis during the day and respiration at night[55]. Given the average temperature of ~ 27 °C and daily temperature fluctuations, the conditions in the ELSS were most comparable to conditions observed at shallow coral reef sites during summer months in Australian and North Pacific reefs[34,55]. Due to their close proximity to the equator, water temperature fluctuations at Indo-pacific reefs are less driven by summer and winter patterns but vary as a consequence of (monsoon induced) upwelling[35]. Overall, the temperature conditions within the ELSS were most comparable to the conditions in January, February, August and September of Indonesian reefs[35].

Inorganic nutrients in the water column and sediment pore water (NO_3^-, NO_2^-, NH_4^+ and PO_4^{3-}) remained low (< 0.2, < 0.01, < 0.15 and < 0.05 mg L^{-1}, respectively) throughout the experiment. Inorganic nutrient concentrations below these values were previously observed in pacific coral reefs as well[56]. Porewater sulphate concentrations of surface sediments have been observed to vary between 2300–2880 mg L^{-1} [57,58]. At the first time point, sulphate was relatively high (2940.0 ± 16.33 mg L^{-1}) in the microcosms, but fell to levels previously observed in coral reef environments[57,58]. Although we detected relatively low DOC in the ELSS at the beginning of the experiment (1.77 ± 0.18 mg C L^{-1}), DOC concentrations increased to 4.97 ± 2.59 mg C L^{-1} at day 34. These values were in the range of DOC concentrations (~ 3 to 8 mg C L^{-1}) in surface sediment pore water at Great Barrier Reef sites (measured using 0.4 µm membrane filters)[59]. It should also be noted that the membrane pore size of our samplers was 0.6 µm, which included a slightly larger fraction of total organic matter compared to the measurements taken at the Great Barrier Reef.

The photosynthetic efficiency of *M. capricornis*, *S. glaucum* and *Zoanthus* sp. did not change significantly following 34 days in the microcosms, which indicates that the photo-physiology of these organisms was stable. The photosynthetic efficiency of *M. digitata*, however, was significantly higher at day 34 compared to Pre conditions. The increased photosynthetic efficiency can indicate a certain level of photo-acclimation of the photosynthetic endosymbionts of *M. digitata* to the light conditions in the ELSS[60,61]. The photosynthetic efficiency may also vary due to shifts in auto- versus heterotrophic feeding ratios, influenced by factors such as organic matter availability.

ELSS bacterial communities

Community composition and diversity

In line with previous studies, our analysis showed that bacterial evenness and richness were lowest in the sponge *Chondrilla* sp. and highest in the sediment[62,63]. In both water and sediment, there were significant shifts in bacterial evenness, and composition from day 8 to 29, but not from day 29 to 34, suggesting microbiome stabilization. Additionally, sediment bacterial evenness declined significantly from Pre to day 8 and subsequently increased from day 8 to 29 and 34. Sediment bacterial richness, however, significantly declined from day 29 to 34. Previously, Coelho et al.[14] also observed lower bacterial richness in microcosms compared to natural sediment. They attributed this to the more stable and less heterogeneous conditions in microcosms. Community composition in Pre sediments was compositionally distinct from all ELSS sediments. The PCO analysis showed, however, that communities at day 29 and 34 deviated less from Pre than day 8 communities. Note that some community variation in Pre compared to microcosm sediments might also be related to the use of different preservation methods (96% alcohol and immediate freezing, respectively)[64,65].

Bacterial richness and evenness in the present study fell within ranges observed at natural reef sites for all host-associated biotopes with the exception of *Zoanthus* sp., where relatively low richness values were observed compared to previous findings[66–68]. Richness and evenness at specific time points varied more among individuals of hard and soft coral biotopes than among individuals of the sponge *Chondrilla* sp., in line with previous in situ comparisons of corals and sponges[63]. Evenness only differed significantly between sampling events (Pre and day 34) in *M. digitata*, increasing substantially from Pre to day 34. Bacterial composition, in turn, differed significantly between Pre and day 34 for *M. digitata* and *Chondrilla* sp., but not for the other host-associated biotopes. This finding suggests that the bacterial communities of *M. digitata* and *Chondrilla* sp. were responsive to changing environmental conditions as exemplified in the present case by transplantation between aquaria. Previous studies have shown that the bacterial communities of certain coral species change along with shifting environmental conditions, a trait, which may be part of the process of host adaptation to new environmental conditions[24,70,71]. Moreover, we found Pre host-specific and Pre sediment-specific ASVs in both the bacterial communities of the hosts and the sediment at day 34, suggesting bacterial exchange between biotopes in the ELSS. In reef environments, host-associated biotopes were also found to share a significant percentage of ASVs with sediments[33]. Our findings suggest a mutual exchange, where members from the sediment community colonize hosts and vice versa. Overall community variance among host individuals, however, was similar in Pre compared to day 34 conditions and samples clustered according to their respective host species in both conditions. This indicates that the bacterial communities of individuals of the same species maintained their relatedness despite their cultivation in separate aquaria for 34 days.

Bacterial higher taxonomic composition

Dominant classes and phyla observed in the present study were similar to those observed in situ in several coral reef studies[33,62,67,69]. Across biotopes, the most abundant higher taxa consisted of Alpha- and Gammaproteobacteria, Bacteriodota, Verrucomicrobiota (with exception of sponges) and Planctomycetota (with the exception of water and sponges). Firmicutes were most abundant in corals, whereas Cyanobacteria, Acidobacteriota and Gemmatimonadota were most abundant in sponges and Patescibacteria in water. In sediment and water, the abundance of several higher taxonomic groups differed significantly among sampling events, whereas no significant variation was observed among host organisms. In sediment, the relative abundance of the phylum Desulfobactereota was significantly higher in Pre compared to days 8, 29 and 34. Bacterial members of this phylum were mainly assigned to the orders Desulfobulbales, Desulfobacterales and Sva1033. These orders include a variety of presumably, anearobic sulfate-reducing bacteria, which are widespread and abundant in marine sediments where they oxidize organic matter by reducing sulfate to sulfide under anoxic conditions[72–74]. This finding indicates that the microcosm sediment layers may have been exposed to higher oxygen concentrations than sediment retrieved from coral reefs, thereby favouring aerobic (e.g., Rhodobacteraceae members) groups. Longer incubation times might be needed for the re-establishment of anaerobic sediment regions. The abundance of the phylum Chloroflexi was significantly lower at day 8 compared to Pre, but increased to abundances similar to Pre at later time points. Although not significant, the same pattern was observed for Acidobacteriota and Gemmatimonadota, and indicates recolonization by these bacterial groups after an initial disturbance. In water, the relative abundance of Verrucomicrobiota and Planctomycetota increased from day 8 to day 29 and day 34. Members of these bacterial phyla are often observed within marine bacterioplankton communities where they have been associated with microalgal blooms[75,76]. Recently, genomic and proteomic data indicated that small, coccoid, free-living Verrucomicrobiota specialise in the degradation of fucoidan-like substrates during spring algal blooms in the North Sea[73].

Most abundant ASVs and closely related organisms

In sediment, abundant ASVs were assigned to the genera *Ruegeria* (family Rhodobacteraceae), *Methyloceanibacter* (family Methyloligellaceae) and *Filomicrobium* (family Hyphomicrobiaceae). Members of these families were previously found to be abundant in marine sediment and are known to play an important role in nutrient remineralization[26,72,77,78]. Recently, *Ruegeria* strains isolated from marine sediment were observed to utilize various organic and inorganic compounds, oxidize sulfur, and perform complete denitrification by reducing nitrate to molecular nitrogen[77]. The Methyloligellaceae and Hyphomicrobiaceae families include bacterial species, which are able to reduce one-carbon compounds (methylotrophs) and oxidize methane under aerobic conditions[78]. Additionally, *Methyloceanibacter* members may be involved in nitrogen cycling[72,78].

ASV-2, assigned to the Rhodobacteraceae, was particularly abundant in water and had 100% sequence similarity to an organism identified as *Tritonibacter litoralis* isolated from coastal surface seawater[79]. *Tritonibacter*

members are globally distributed and primarily found in surface waters[80]. They are also often found in association with seaweeds due to their ability to metabolize dimethylsulfoniopropionate (DMSP)[79,80]. Moreover, certain *Tritonibacter* strains (producers of the antibacterial compound Tropodithietic acid) can inhibit the growth of fast-growing bacteria and fish pathogens[81]. ASV-33, assigned to the Pirellulaceae, was abundant in all cnidarian biotopes in the present study, but absent from other biotopes. Members of this family have previously been detected in deep-sea octocorals and sponges and are believed to play a role in nitrogen cycling[82,83]. ASV-10, assigned to the genus *Endozoicomonas*, was only recorded in *Zoanthus* sp.. *Endozoicomonas* spp. have been recorded across a range of hosts including corals. Previous studies have suggested that they play important roles in host nutrient cycling and influence microbiome structure[84,85]. ASVs 1 and 32, assigned to the Ca. *Synechococcus spongiarum*, were specifically enriched in *Chondrilla* sp.. Members of this genus have been previously detected in 28 sponge species and may play a role in carbon assimilation and transfer to their sponge host[86,87]. ASVs 18 and 42, assigned to the Ca. *Hepatoplasma* (Tenericutes) were only detected in *S. glaucum*. Members of this genus have been suggested to play roles in the degradation of complex organic molecules in the digestive tracts of terrestrial and marine isopods[88]. Notably, three ASVs assigned to the phylum Patescibacteria (ASVs 30, 43, 186) were found across a variety of biotopes from day 29 onward, but were not detected in natural sediment or host-associated bacterial communities sampled prior to addition to the ELSS (Pre). Patescibacteria currently lack isolated representatives but have been detected in marine surface water[89], sediment[88] and reef sponges[91]. Members of this phylum are characterized by reduced cell and genome sizes with limited metabolic capacities[92]. It has been suggested that they live in symbiosis with other bacteria[93] and presumably play a role in oceanic carbon cycling, a finding substantiated by the detection of genes required for carbon fixation in nano-sized patescibacterial members[94].

Putative functional profiles of bacterial communities

Despite some variation among biotopes, the predicted functional profiles (e.g., degradation of aromatic compounds, nutrient metabolism, and biosynthesis of secondary metabolites and antibiotics) of bacterial communities in water, sediment and host biotopes were relatively uniform at different sampling events. The predicted gene counts of the cAMP signalling and two-component system categories were, however, significantly lower at all time points from day 8 onward in the sediment biotope compared to Pre, whereas the reverse held for the quorum sensing category. The two-component system and cAMP signalling categories help bacteria to adapt to changing environmental conditions[95–97]. Quorum sensing, in turn, allows groups of bacteria to synchronously alter gene expression in response to changes in population density and environmental cues[98]. In addition, quorum sensing has been predicted to give bacteria a competitive advantage under nutrient limiting conditions[99]. These conditions were likely present during the early stages of the experiment (day 8) and match the prevalence of the quorum sensing pathway. Previous studies have shown that the two-component system category was enriched in members of the phylum Desulfobacterota[100], whereas, the quorum sensing category was enriched in members of the class Alphaproteobacteria[101–103]. These findings suggest an association between higher taxonomic abundance and predicted function. Note that the predictive functional profiles only included ASVs of which metagenomic data was available in the database, as opposed to presenting a complete view of the functional pathway abundance in the dataset.

Conclusion

The current study described and validated an ELSS to study host and free-living coral reef bacterial communities. The physical and chemical conditions and bacterial communities of the ELSS were similar to those of coral reef ecosystems. Sediment bacterial diversity and composition were more similar between Pre and day 29 and day 34 than between Pre and day 8. These results suggest that a recovery period is necessary for ELSS setups before meaningful comparisons to environmental conditions can be made. Similarities between Pre and day 29 and day 34 communities suggest an adequate recovery period occurred in the presented setup. By changing the pre-sets of our ELSS values with respect to temperature and UV, it is possible to simulate several scenarios of global climate change, such as the predicted increase in temperature and UVB. Temperature can be regulated using water-baths, which allow temperature control in blocks of four independent microcosms. The transparent polyester films that blocked UVB radiation in our validation trial can be removed from individual microcosms. Additionally, irradiance values can be manipulated by varying lamp intensity and time of operation. The modular design of the ELSS developed here offers a multitude of statistically robust experimental designs. In this way, the system enables researchers to establish cause–effect relationships of the individual and interactive effects of a suite of environmental conditions on marine bacterial communities.

Data availability

Sequences generated in this study can be downloaded from the NCBI Sequence Read Archive under the BioProject accession number PRJNA904682.

Received: 26 July 2023; Accepted: 6 August 2024
Published online: 11 September 2024

References

1. Fisher, R. *et al.* Species richness on coral reefs and the pursuit of convergent global estimates. *Curr. Biol.* **25**, 500–505 (2015).
2. Moberg, F. & Folke, C. Ecological goods and services of coral reef ecosystems. *Ecol. Econ.* **29**, 215–233 (1999).
3. Plaisance, L., Caley, M. J., Brainard, R. E. & Knowlton, N. The diversity of coral reefs: What are we missing?. *PLoS One* **6**, e25026 (2011).

4. Baker, A. C., Glynn, P. W. & Riegl, B. Climate change and coral reef bleaching: An ecological assessment of long-term impacts, recovery trends and future outlook. *Estuar. Coast. Shelf Sci.* **80**, 435–471 (2008).
5. De'ath, G., Fabricius, K. E., Sweatman, H. & Puotinen, M. The 27-year decline of coral cover on the Great Barrier Reef and its causes. *Proc. Natl. Acad. Sci.* **109**, 17995–17999 (2012).
6. Glynn, P. W., Manzello, D. P. & Enochs, I. C. *Coral Reefs of the Eastern Tropical Pacific. Persistence and Loss in a Dynamic Environment. Coral Reefs* Vol. 15 (Springer, 2015).
7. Cai, W. *et al.* ENSO and greenhouse warming. *Nat. Clim. Chang.* **5**, 849–859 (2015).
8. Wang, B. *et al.* Historical change of El Niño properties sheds light on future changes of extreme El Niño. *Proc. Natl. Acad. Sci. U. S. A.* **116**, 22512–22517 (2019).
9. Ying, J. *et al.* Emergence of climate change in the tropical Pacific. *Nat. Clim. Chang.* **12**, 356–364 (2022).
10. Eakin, C. M., Sweatman, H. P. A. & Brainard, R. E. The 2014–2017 global-scale coral bleaching event: Insights and impacts. *Coral Reefs* **38**, 539–545 (2019).
11. McGowan, H. & Theobald, A. ENSO weather and coral bleaching on the Great Barrier Reef, Australia. *Geophys. Res. Lett.* **44**, 10601–10607 (2017).
12. Masson-Delmotte, V. *et al.* Climate change 2021: the physical science basis. *Contrib. Work. Gr. I to sixth Assess. Rep. Intergov. panel Clim. Chang.* 2 (2021).
13. Dizon, R. T. & Yap, H. T. Understanding coral reefs as complex systems: Degradation and prospects for recovery. *Sci. Mar.* **70**, 219–226 (2006).
14. Coelho, F. J. R. C. *et al.* Development and validation of an experimental life support system for assessing the effects of global climate change and environmental contamination on estuarine and coastal marine benthic communities. *Glob. Chang. Biol.* **19**, 2584–2595 (2013).
15. Coelho, F. J. R. C. *et al.* Unraveling the interactive effects of climate change and oil contamination on laboratory-simulated estuarine benthic communities. *Glob. Chang. Biol.* **21**, 1871–1886 (2015).
16. Findlay, H. S., Kendall, M. A., Spicer, J. I., Turley, C. & Widdicombe, S. Novel microcosm system for investigating the effects of elevated carbon dioxide and temperature on intertidal organisms. *Aquat. Biol.* **3**, 51–62 (2008).
17. Schubert, P. & Wilke, T. Coral microcosms: Challenges and opportunities for global change biology. *Corals Chang. World* **395**, 144–175. https://doi.org/10.1016/j.colsurfa.2011.12.014 (2018).
18. Boyd, P. W. *et al.* Experimental strategies to assess the biological ramifications of multiple drivers of global ocean change—A review. *Glob. Chang. Biol.* **24**, 2239–2261 (2018).
19. Courtial, L. *et al.* Effects of temperature and UVR on organic matter fluxes and the metabolic activity of *Acropora muricata*. *Biol. Open* **6**, 1190–1199 (2017).
20. Schlöder, C. & D'Croz, L. Responses of massive and branching coral species to the combined effects of water temperature and nitrate enrichment. *J. Exp. Mar. Bio. Ecol.* **313**, 255–268 (2004).
21. Ainsworth, T. D., Thurber, R. V. & Gates, R. D. The future of coral reefs: A microbial perspective. *Trends Ecol. Evol.* **25**, 233–240 (2010).
22. Glasl, B. *et al.* Microbial predictors of environmental perturbations in coral reef ecosystems. *bioRxiv* 1–13 (2019) https://doi.org/10.1101/524173.
23. van Oppen, M. J. H. & Blackall, L. L. Coral microbiome dynamics, functions and design in a changing world. *Nat. Rev. Microbiol.* **17**, 557–567 (2019).
24. Vanwonterghem, I. & Webster, N. S. Coral reef microorganisms in a changing climate. *iScience* **23**, 100972 (2020).
25. Alongi, D. M. The role of bacteria in nutrient recycling in tropical mangrove and other coastal benthic ecosystems. In *Ecology and conservation of southeast Asian marine and freshwater environments including wetlands* 19–32 (Springer, 1994).
26. Dong, X. *et al.* Metagenomic views of microbial communities in sand sediments associated with coral reefs. *Microb. Ecol.* **85**, 465–477 (2022).
27. Rädecker, N., Pogoreutz, C., Voolstra, C. R., Wiedenmann, J. & Wild, C. Nitrogen cycling in corals: The key to understanding holobiont functioning?. *Trends Microbiol.* **23**, 490–497 (2015).
28. Ricci, F. *et al.* Beneath the surface: Community assembly and functions of the coral skeleton microbiome. *Microbiome* **7**, 1–10 (2019).
29. Rosenberg, E., Koren, O., Reshef, L., Efrony, R. & Zilber-Rosenberg, I. The role of microorganisms in coral health, disease and evolution. *Nat. Rev. Microbiol.* **5**, 355–362 (2007).
30. Wild, C. *et al.* Degradation and mineralization of coral mucus in reef environments. *Mar. Ecol. Prog. Ser.* **267**, 159–171 (2004).
31. Fan, L., Liu, M., Simister, R., Webster, N. S. & Thomas, T. Marine microbial symbiosis heats up: The phylogenetic and functional response of a sponge holobiont to thermal stress. *ISME J.* **7**, 991–1002 (2013).
32. McDevitt-Irwin, J. M., Baum, J. K., Garren, M. & Vega Thurber, R. L. Responses of coral-associated bacterial communities to local and global stressors. *Front. Mar. Sci.* **4**, 1–16 (2017).
33. Cleary, D. F. R. *et al.* The sponge microbiome within the greater coral reef microbial metacommunity. *Nat. Commun.* **10**, 1–12 (2019).
34. Bainbridge, S. J. Temperature and light patterns at four reefs along the Great Barrier Reef during the 2015–2016 austral summer: Understanding patterns of observed coral bleaching. *J. Oper. Oceanogr.* **10**, 16–29 (2017).
35. Kusuma, D. W. *et al.* Sea surface temperature dynamics in Indonesia. *IOP Conf. Ser. Earth Environ. Sci.* **98**, 012038 (2017).
36. Müller, R., Wiencke, C., Bischof, K. & Krock, B. Zoospores of three arctic laminariales under different UV radiation and temperature conditions: Exceptional spectral absorbance properties and lack of phlorotannin induction. *Photochem. Photobiol.* **85**, 970–977 (2009).
37. Zacher, K., Hanelt, D., Wiencke, C. & Wulff, A. Grazing and UV radiation effects on an Antarctic intertidal microalgal assemblage: A long-term field study. *Polar Biol.* **30**, 1203–1212 (2007).
38. Otte, J. M. *et al.* Sterilization impacts on marine sediment-Are we able to inactivate microorganisms in environmental samples?. *FEMS Microbiol. Ecol.* **94**, 1–14 (2018).
39. Rocha, R. J. M. *et al.* Development of a standardized modular system for experimental coral culture. *J. World Aquac. Soc.* **46**, 235–251 (2015).
40. Maxwell, K. & Johnson, G. N. Chlorophyll fluorescence—A practical guide. *J Exp Bot* **51**, 659–668 (2018).
41. Downs, C. A. *et al.* Oxidative stress and seasonal coral bleaching. *Free Radic. Biol. Med.* **33**, 533–543 (2002).
42. Torti, A., Lever, M. A. & Jørgensen, B. B. Origin, dynamics, and implications of extracellular DNA pools in marine sediments. *Mar. Genomics* **24**, 185–196 (2015).
43. Hornung, B. V. H., Zwittink, R. D. & Kuijper, E. J. Issues and current standards of controls in microbiome research. *FEMS Microbiol. Ecol.* **95**, 1–7 (2019).
44. Bolyen, E. *et al.* Reproducible, interactive, scalable and extensible microbiome data science using QIIME 2. *Nat. Biotechnol.* **37**, 852–857 (2019).
45. Callahan, B. J. *et al.* DADA2: High-resolution sample inference from Illumina amplicon data. *Nat. Methods* **13**, 581–583 (2016).
46. Glassing, A., Dowd, S. E., Galandiuk, S., Davis, B. & Chiodini, R. J. Inherent bacterial DNA contamination of extraction and sequencing reagents may affect interpretation of microbiota in low bacterial biomass samples. *Gut Pathog.* **8**, 1–12 (2016).

47. Salter, S. J. *et al.* Reagent and laboratory contamination can critically impact sequence-based microbiome analyses. *BMC Biol.* **12**, 1–12 (2014).
48. Weyrich, L. S. *et al.* Laboratory contamination over time during low-biomass sample analysis. *Mol. Ecol. Resour.* **19**, 982–996 (2019).
49. Wemheuer, F. *et al.* Tax4Fun2: Prediction of habitat-specific functional profiles and functional redundancy based on 16S rRNA gene sequences. *Environ. Microbiomes* **15**, 1–12 (2020).
50. Zhang, Z., Schwartz, S., Wagner, L. & Miller, W. A greedy algorithm for aligning DNA sequences. *J. Comput. Biol.* **7**, 203–214 (2000).
51. Oksanen, J. *et al.* vegan: Community ecology package. R package version 2.5–6. (2019).
52. Lenth, R., Singmann, H., Love, J., Buerkner, P. & Herve, M. emmeans : Estimated Marginal Means, aka Least-Squares Means. *R package version 1.15–15* (2020) https://doi.org/10.1080/00031305.1980.10483031>.License.
53. Legendre, P. & Gallagher, E. D. Ecologically meaningful transformations for ordination of species data. *Oecologia* **129**, 271–280 (2001).
54. DeCarlo, T. M. *et al.* Mass coral mortality under local amplification of 2 °c ocean warming. *Sci. Rep.* **7**, 1–9 (2017).
55. Guadayol, Ò., Silbiger, N. J., Donahue, M. J. & Thomas, F. I. M. Patterns in temporal variability of temperature, oxygen and pH along an environmental gradient in a coral reef. *PLoS One* **9**, e85213 (2014).
56. Silbiger, N. J. *et al.* Nutrient pollution disrupts key ecosystem functions on coral reefs. *Proc. R. Soc. B* **285**, 20172718 (2018).
57. Alongi, D. M. Effect of monsoonal climate on sulfate reduction in coastal sediments of the central Great Barrier Reef lagoon. *Mar. Biol.* **122**, 497–502 (1995).
58. Werner, U. *et al.* Spatial patterns of aerobic and anaerobic mineralization rates and oxygen penetration dynamics in coral reef sediments. *Mar. Ecol. Prog. Ser.* **309**, 93–105 (2006).
59. Lourey, M. J., Alongi, D. M., Ryan, D. A. J. & Devlin, M. J. Variability of nutrient regeneration rates and nutrient concentrations in surface sediments of the northern Great Barrier Reef shelf. *Cont. Shelf Res.* **21**, 145–155 (2001).
60. Roth, M. S., Latz, M. I., Goericke, R. & Deheyn, D. D. Green fluorescent protein regulation in the coral acropora yongei during photoacclimation. *J. Exp. Biol.* **213**, 3644–3655 (2010).
61. Roth, M. S. The engine of the reef: Photobiology of the coral-algal symbiosis. *Front. Microbiol.* **5**, 1–22 (2014).
62. Cleary, D. F. R. *et al.* A comparison of prokaryote communities inhabiting sponges, bacterial mats, sediment and seawater in Southeast Asian coral reefs. *FEMS Microbiol. Ecol.* **95**, 1–14 (2019).
63. Cleary, D. F. R. *et al.* Bacterial composition of sponges, sediment and seawater in enclosed and open marine lakes in Ha Long Bay Vietnam. *Mar. Biol. Res.* **16**, 18–31 (2020).
64. Tatangelo, V., Franzetti, A., Gandolfi, I., Bestetti, G. & Ambrosini, R. Effect of preservation method on the assessment of bacterial community structure in soil and water samples. *FEMS Microbiol. Letters* **356**(1), 32–38 (2014).
65. Dully, V. *et al.* Comparing sediment preservation methods for genomic biomonitoring of coastal marine ecosystems. *Mar. Pollut. Bull.* **173**, 113129 (2021).
66. Cai, L. *et al.* Exploring coral microbiome assemblages in the South China Sea. *Sci. Rep.* **8**, 1–13 (2018).
67. O'Brien, P. A. *et al.* Diverse coral reef invertebrates exhibit patterns of phylosymbiosis. *ISME J.* **14**, 2211–2222 (2020).
68. Shore-Maggio, A., Runyon, C. M., Ushijima, B., Aeby, G. S. & Callahan, S. M. Differences in bacterial community structure in two color morphs of the Hawaiian reef coral Montipora capitata. *Appl. Environ. Microbiol.* **81**, 7312–7318 (2015).
69. Sun, W., Zhang, F., He, L. & Li, Z. Pyrosequencing reveals diverse microbial community associated with the Zoanthid *Palythoa australiae* from the South China Sea. *Microb. Ecol.* **67**, 942–950 (2014).
70. Lurgi, M., Thomas, T., Wemheuer, B., Webster, N. S. & Montoya, J. M. Modularity and predicted functions of the global sponge-microbiome network. *Nat. Commun.* **10**, 992 (2019).
71. Ziegler, M. *et al.* Coral bacterial community structure responds to environmental change in a host-specific manner. *Nat. Commun.* **10**, 3092 (2019).
72. Begmatov, S. *et al.* Microbial communities involved in methane, sulfur, and nitrogen cycling in the sediments of the barents sea. *Microorganisms* **9**, 1–21 (2021).
73. Rabus, R. *et al.* A post-genomic view of the ecophysiology, catabolism and biotechnological relevance of sulphate-reducing prokaryotes. *Adv. Microb. Physiol.* **66**, 55–321 (2015).
74. Zoppini, A. *et al.* Corrigendum to "Bacterial diversity and microbial functional responses to organic matter composition and persistent organic pollutants in deltaic lagoon sediment" [Estuar. Coast Shelf Sci. 233 (5 February 2020) 106508] (Estuarine, Coastal and Shelf Scienc. *Estuar. Coast. Shelf Sci.* **237**, 106606 (2020).
75. Orellana, L. H. *et al.* Verrucomicrobiota are specialist consumers of sulfated methyl pentoses during diatom blooms. *ISME J.* **16**, 630–641 (2022).
76. Wiegand, S., Jogler, M. & Jogler, C. On the maverick planctomycetes. *FEMS Microbiol. Rev.* **42**, 739–760 (2018).
77. Lin, X., Mcnichol, J., Chu, X., Qian, Y. & Luo, H. Cryptic niche differentiation of novel sediment ecotypes of *Ruegeria pomeroyi* correlates with nitrate respiration. *Environ. Microbiol.* **24**, 390–403 (2022).
78. Vekeman, B. *et al.* New Methyloceanibacter diversity from North Sea sediments includes methanotroph containing solely the soluble methane monooxygenase. *Environ. Microbiol.* **18**, 4523–4536 (2016).
79. Li, N. *et al. Tritonibacter aquimaris* sp. nov. and *Tritonibacter litoralis* sp. nov., two novel members of the Roseobacter group isolated from coastal seawater. *Antonie Van Leeuwenhoek* **114**, 787–798 (2021).
80. Brinkhoff, T., Giebel, H. A. & Simon, M. Diversity, ecology, and genomics of the *Roseobacter* clade: A short overview. *Arch. Microbiol.* **189**, 531–539 (2008).
81. Henriksen, N. N. S. E. *et al.* Role is in the eye of the beholder—The multiple functions of the antibacterial compound tropodithietic acid produced by marine Rhodobacteraceae. *FEMS Microbiol. Rev.* **46**, 1–15 (2022).
82. Kellogg, C. A., Ross, S. W. & Brooke, S. D. Bacterial community diversity of the deep-sea octocoral *Paramuricea placomus*. *PeerJ* **4**, e2529 (2016).
83. Mohamed, N. M., Saito, K., Tal, Y. & Hill, R. T. Diversity of aerobic and anaerobic ammonia-oxidizing bacteria in marine sponges. *ISME J.* **4**, 38–48 (2010).
84. Neave, M. J., Apprill, A., Ferrier-Pagès, C. & Voolstra, C. R. Diversity and function of prevalent symbiotic marine bacteria in the genus *Endozoicomonas*. *Appl. Microbiol. Biotechnol.* **100**, 8315–8324 (2016).
85. Pogoreutz, C. *et al.* Coral holobiont cues prime *Endozoicomonas* for a symbiotic lifestyle. *ISME J.* **16**, 1883–1895 (2022).
86. Burgsdorf, I. *et al.* Lifestyle evolution in cyanobacterial symbionts of sponges. *MBio* **6**, 391–406 (2015).
87. Burgsdorf, I. *et al.* Lineage-specific energy and carbon metabolism of sponge symbionts and contributions to the host carbon pool. *ISME J.* **16**, 1163–1175 (2022).
88. Bouchon, D., Zimmer, M. & Dittmer, J. The terrestrial isopod microbiome: An all-in-one toolbox for animal-microbe interactions of ecological relevance. *Front. Microbiol.* **7**, 1472 (2016).
89. Rahlff, J. *et al.* Overlooked diversity of ultramicrobacterial minorities at the air-sea interface. *Atmosphere (Basel).* **11**, 1–19 (2020).
90. Demko, A. M., Patin, N. V. & Jensen, P. R. Microbial diversity in tropical marine sediments assessed using culture-dependent and culture-independent techniques. *Environ. Microbiol.* https://doi.org/10.1111/1462-2920.15798 (2021).
91. Robbins, S. J. *et al.* A genomic view of the microbiome of coral reef demosponges. *ISME J.* **15**, 1641–1654 (2021).
92. Brown, C. T. *et al.* Unusual biology across a group comprising more than 15% of domain Bacteria. *Nature* **523**, 208–211 (2015).

93. Lemos, L. N. *et al.* Genomic signatures and co-occurrence patterns of the ultra-small Saccharimonadia (phylum CPR/Patescibacteria) suggest a symbiotic lifestyle. *Mol. Ecol.* **28**, 4259–4271 (2019).
94. Lannes, R., Olsson-Francis, K., Lopez, P. & Bapteste, E. Carbon fixation bymarine ultrasmall prokaryotes. *Genome Biol. Evol.* **11**, 1166–1177 (2019).
95. Ohmori, K., Ehira, S., Kimura, S. & Ohmori, M. Changes in the amount of cellular trehalose, the activity of maltooligosyl trehalose hydrolase, and the expression of its gene in response to salt stress in the cyanobacterium *Spirulina platensis*. *Microbes Environ.* **24**, 52–56 (2009).
96. You, C. *et al.* Coordination of bacterial proteome with metabolism by cyclic AMP signalling. *Nature* **500**, 301–306 (2013).
97. Zschiedrich, C. P., Keidel, V. & Szurmant, H. Molecular mechanisms of two-component signal transduction. *J. Mol. Biol.* **428**, 3752–3775 (2016).
98. Mukherjee, S. & Bassler, B. L. Bacterial quorum sensing in complex and dynamically changing environments. *Nat. Rev. Microbiol.* **17**, 371–382 (2019).
99. Schluter, J., Schoech, A. P., Foster, K. R., Mitri, S. & Locke, J. C. The Evolution of Quorum sensing as a mechanism to Infer Kinship. *PLoS Comput. Biol.* **12**, 1004848 (2016).
100. Alm, E., Huang, K. & Arkin, A. The Evolution of Two-Component Systemsin Bacteria Reveals Different Strategiesfor Niche Adaptation. *Plos Comput. Biol.* **2**, e143 (2006).
101. Armes, A. C. & Buchan, A. Cyclic di-GMP is integrated into a hierarchal quorum sensing network regulating antimicrobial production and biofilm formation in *Roseobacter* clade member Rhodobacterales Strain Y4I. *Front. Mar. Sci.* https://doi.org/10.3389/fmars.2021.681551 (2021).
102. Cude, W. N. & Buchan, A. Acyl-homoserine lactone-based quorum sensing in the *Roseobacter* clade: Complex cell-to-cell communication controls multiple physiologies. *Front. Microbiol.* **4**, 1–12 (2013).
103. Zan, J., Liu, Y., Fuqua, C. & Hill, R. T. Acyl-homoserine lactone quorum sensing in the *Roseobacter* clade. *Int. J. Mol. Sci.* **15**, 654–669 (2014).

Acknowledgements

We are grateful to F. Coelho and V. Oliveira for their help during lab work and FOLEX COATING GMBH in Germany for providing samples of their specialized polyester film. Also, we are thankful to J. Hilgendorf for her assistance in the creation of Fig. 2. The research was conducted at the Laboratory of Molecular Studies and Marine Environment, situated at the Centre for Environmental and Marine Studies (CESAM), University of Aveiro, Portugal.

Author contributions

T.M.S: Methodology, Investigation, Data analysis, Writing—original draft, review & editing; D.F.R.C: Supervision, Conceptualization, Data analysis, Writing—original draft, review & editing; R.J.M.R.: Resources, Conceptualization, Writing—review & editing; A.R.M.P.: Investigation, Writing—review & editing; D.A.M.S.: Conceptualization, Investigation, Writing—review & editing; J.C.F.: Resources, Writing—review & editing; A.L.: Conceptualization, Methodology, Investigation, Writing—review & editing; Y.M.H.: Resources, Writing—review & editing; N.J.dV: Supervision, Conceptualization, Resources, Writing—review & editing; N.C.M.G.: Supervision, Conceptualization, Resources, Methodology, Writing—original draft, review & editing.

Funding

This study is funded by 4D-REEF (www.4d-reef.eu). 4D-REEF receives funding from the European Union's Horizon 2020 research and innovation program under the Marie Sklodowska-Curie grant agreement No 813360. Additional funding was received from the Ministry of Science and Technology, Taiwan to Y. M. Huang (MOST 110-2621-B-346-001). Ana R.M. Polónia was supported by a postdoctoral scholarship (SFRH/BPD/117563/2016) funded by the Portuguese Foundation for Science and Technology (FCT)/national funds (MCTES) and by the European Social Fund (ESF)/EU. Davide A.M. Silva was supported by a PhD grant (2020.05774.BD) funded by the Portuguese Foundation for Science and Technology (FCT), national funds (MCTES), and the European Social Fund POPH-QREN programme. Jörg C. Frommlet was supported by national funds (OE), through FCT, in the scope of the framework contract foreseen in the numbers 4, 5 and 6 of the article 23, of the Decree-Law 57/2016, of August 29, changed by Law 57/2017, of July 19. We acknowledge financial support to CESAM by FCT/MCTES (UIDP/50017/2020 + UIDB/50017/2020 + LA/P/0094/2020), through national funds. Additional funding was received from the research programme NWO-VIDI with project number 16.161.301, which is financed by the Netherlands Organisation for Scientific Research (NWO).

Competing interests

The authors declare no competing interests.

Additional information

Supplementary Information The online version contains supplementary material available at https://doi.org/10.1038/s41598-024-69514-0.

Correspondence and requests for materials should be addressed to T.M.S. or N.C.M.G.